The American Journal of Pathology, Vol. 193, No. 4, April 2023

The American Journal of
PATHOLOGY
ajp.amjpathol.org

IMMUNOPATHOLOGY AND INFECTIOUS DISEASES

Inflammation-Associated Lung Tissue Remodeling and Fibrosis in Morphine-Dependent SIV-Infected Macaques

Divya T. Chemparathy,* Susmita Sil,* Shannon Callen,* Hitendra S. Chand,† Mohan Sopori,‡ Todd A. Wyatt,§¶‖ Arpan Acharya,* Siddappa N. Byrareddy,* Howard S. Fox,** and Shilpa Buch*

From the Departments of Pharmacology and Experimental Neuroscience, Internal Medicine,‖ and Neurological Sciences,** College of Medicine, and the Department of Environmental, Agricultural and Occupational Health,¶ College of Public Health, University of Nebraska Medical Center, Omaha, Nebraska; the Department of Immunology and Nano-Medicine,† Alzheimer's Disease Research Unit, Herbert Wertheim College of Medicine, Florida International University, Miami, Florida; the Respiratory Immunology Division,‡ Lovelace Respiratory Research Institute, Albuquerque, New Mexico; and the Veterans Affairs Nebraska–Western Iowa Health Care System,§ Omaha, Nebraska*

Accepted for publication December 20, 2022.

Address correspondence to Shilpa Buch, Ph.D., Department of Pharmacology and Experimental Neuroscience, University of Nebraska Medical Center, 42nd and Emile, Omaha, NE 68198.
E-mail: sbuch@unmc.edu.

With the advent of antiretroviral therapy, improved survival of people with HIV (PWH) is accompanied with increased prevalence of HIV-associated comorbidities. Chronic lung anomalies are recognized as one of the most devastating sequelae in PWH. The limited available data describing the lung complications in PWH with a history of opioid abuse warrants more research to better define the course of disease pathogenesis. The current study was conducted to investigate the progression of lung tissue remodeling in a morphine (Mor)–exposed rhesus macaque model of SIV infection. Pathologic features of lung remodeling, including histopathologic changes, oxidative stress, inflammation, and proliferation of fibroblasts, were investigated in archival lung tissues of SIVmac-251/macaque model with or without Mor dependence. Lungs of Mor-exposed, SIV-infected macaques exhibited significant fibrotic changes and collagen deposition in the alveolar and the bronchiolar region. There was increased oxidative stress, profibrotic transforming growth factor-β, fibroblast proliferation and transdifferentiation, epithelial-mesenchymal transition, and matrix degradation in SIV-infected macaques, which was further exacerbated in the lungs of Mor-exposed macaques. Interestingly, there was decreased inflammation-associated remodeling in Mor-dependent SIV-infected macaques compared with SIV-infected macaques that did not receive Mor. Thus, the current findings suggest that SIV independently induces fibrotic changes in macaque lungs, which is further aggravated by Mor. *(Am J Pathol 2023, 193: 380–391; https://doi.org/10.1016/j.ajpath.2022.12.016)*

Since the discovery of HIV, HIV-associated pulmonary complications have been the prominent cause of morbidity and mortality in people with HIV (PWH).[1] Epidemiologic studies in the era of mono-antiviral therapy showed that the most frequent pulmonary complications among PWH were acute bronchitis, bacterial pneumonia, and *Pneumocystis carinii* pneumonia.[1] Despite the advent of combined antiretroviral therapy, the incidence of chronic obstructive pulmonary disease,[2,3] pulmonary arterial hypertension,[4] chronic bronchitis,[5] and asthma[6] is higher in PWH. A recent multicenter nationwide cohort study has revealed an increased incidence of previously unrecognized pulmonary fibrosis (PF) among HIV-infected patients.[7] However, the role of drug abuse on interstitial lung disease, such as PF or idiopathic PF, remains unexplored, specifically when substance abuse is highly prevalent among PWH, with nearly

Supported by NIH grants R01DA041751 (S.B.) and R01DA035203 (S.B.); and Nebraska Center for Substance Abuse Research.
D.T.C. and S.S. contributed equally to this work and share first authorship.
Disclosures: None declared.

https://doi.org/10.1016/j.ajpath.2022.12.016

50% afflicted with drug abuse—associated comorbidities.[8] A study involving a cohort of 167 HIV-infected patients found that 47.3% of participants had respiratory abnormalities associated with i.v. drug use, of which 21% presented with irreversible airway obstruction.[9]

PF is a progressive fatal lung disease characterized by excessive proliferation of fibroblasts and deposition of extracellular matrix (ECM) that leads to irreversible lung remodeling.[10] Environmental and occupational factors, such as smoking, viral infection, and pollutants, may accelerate pulmonary injury and promote fibrosis.[11] The pathophysiology of PF entails accelerated proliferation and decreased apoptosis of fibroblasts, and increased deposition and decreased breakdown of ECM.[12] The elevated ECM deposition may result from the increased epithelial-mesenchymal transition (EMT).[13] Moreover, HIV-1 and SIV infections promote a massive accumulation of collagen through induction of transforming growth factor-β1 (TGF-β1) in the lymphoid tissues of humans and rhesus macaques.[14,15] Also, SIV infection—induced pulmonary arteriopathy in rhesus macaques and morphine (Mor) dependence potentiate the endothelial injury and the pulmonary vascular remodeling in SIV-infected macaques.[16] Therefore, the current study investigated the pathogenic changes in the lungs of morphine-exposed rhesus macaques after SIV infection. The study presents, for the first time, evidence that SIV infection in rhesus macaques induces histopathologic and lung tissue remodeling manifestations of pulmonary fibrosis that are significantly exaggerated in morphine dependence.

Materials and Methods

Macaques

Archival lung tissues from the male Indian rhesus macaques (*Macaca mulatta*) infected with SIVmac251 exposed to morphine (SIV + Mor group), or infected macaques without morphine dependence (SIV group), or morphine-exposed uninfected controls (Mor group), or saline controls were used for this study. All the Institutional Animal Care and Use Committee guidelines were followed, and the experimental protocols were approved by Institutional Animal Care and Use Committee, University of Nebraska Medical Center. For macaques in Mor group and SIV + Mor group, 45 weeks of morphine injections were administered (72 mg/kg/week, i.m., 12 injections per week). Sham injections of saline were given to macaques in the saline group and SIV group. Macaques in the SIV alone and SIV + Mor groups were infected with SIVmac251 following 9 weeks of morphine administration. Animals were sacrificed at the end of 34 weeks after viral inoculation. The homogenates of the lung regions were used for assessing the expression of different protein and mRNA of interest. Inflated, paraffin-embedded lung tissue sections were used for histopathologic and immunostaining analyses. See online supplement for further details of *Materials and Methods*.

Histopathology and Masson Trichrome Collagen Staining

Formalin-fixed, paraffin-embedded lung tissue sections (5 μm thick) of experimental macaques were deparaffinized in xylene and rehydrated in descending grades of ethanol and deionized water. Standard hematoxylin and eosin staining was performed, and histology was assessed by light microscopy. For collagen assessment in the lung tissues, Masson trichrome stain kit (ab150686; Abcam, Cambridge, MA) was used according to the manufacturer's instructions. Briefly, the deparaffinized sections were treated with Bouin solution at 60°C for 1 hour, followed by staining with Weigert Iron Hematoxylin, Biebrich Scarlet—Acid Fuchsin solution, and Aniline Blue Stain Solution (all from Sigma-Aldrich, St. Louis, MO). Then, 1% acetic acid was used to remove the extra non-specific staining from the section. Black-stained nuclei, red-stained cytoplasm and muscle fibers, and blue-stained collagen were determined by light microscopy.

SIV Lung Viral Load Quantification

SIV RNA concentration in the lung tissue samples was measured by quantitative RT-PCR, as previously described.[17] Briefly, total RNA was extracted from lung tissues using a Qiagen kit (74104; Qiagen, Germantown, MD), according to the manufacturer's instructions. SIV gag RNA was quantified by quantitative RT-PCR using the TaqMan RNA-to-Ct 1-Step kit (4392938; Thermo Fisher Scientific, Waltham, MA) using the following primers: forward, 5′-GTCTGCGTCATCTGGTGCATTC-3′; reverse, 5′-CACTAGGTGTCTCTGCACTATCTGTTTTG-3′; and SIV probe, 5′-/6-carboxyfluorescein (FAM)/CTTCCTCAG/ZEN/TGTGTTTCACTTTCTCTTCTGCG/3IABkFQ-3′.

Immunohistochemistry

Formalin-fixed, paraffin-embedded lung tissue sections (5 μm thick) were deparaffinized in xylene and rehydrated in descending grades of ethanol and deionized water. Followed by antigen retrieval in Tris EDTA buffer (pH 9.0), and blocking with phosphate-buffered saline containing normal 3% goat serum (S-1000; Vector Laboratories, Burlingame, CA), the tissue sections were probed with primary antibodies 4-hydroxynonenal (4HNE; rabbit polyclonal IgG; 1:200 dilution; ab46545; Abcam), TGF-β1 (mouse monoclonal IgG; 1:500 dilution; Ma5-18023; Thermo Fisher Scientific), CD64 (rabbit polyclonal IgG; 1:200 dilution; ab203349; Abcam), Ki-67 (rabbit polyclonal IgG; 1:250 dilution; ab15580; Abcam), α-smooth muscle actin (α-SMA; rabbit polyclonal IgG; 1:500 dilution; ab7817; Abcam), and claudin-5 (rabbit polyclonal IgG; 1:50 dilution; ab15106; Abcam). The immunoprobed tissues were detected with respective fluorescent-conjugated secondary antibodies, and the images were acquired using Zeiss LSM 800 confocal laser-scanning microscope (Carl Zeiss, Inc., Jena, Germany).

ImageJ software version 1.4.3.67 (NIH, Bethesda, MD; *https://imagej.nih.gov/ij*, last accessed December 26, 2022) was used for image quantification.

Western Blot Analysis

Protein expression in experimental samples was analyzed by standard Western blot analysis procedure, as described previously.[18] Briefly, proteins were extracted from lung tissue samples using radioimmunoprecipitation assay lysis buffer containing protease (78429; Thermo Fisher Scientific) and phosphatase (78427; Thermo Fisher Scientific) inhibitors and were quantified by using Pierce BCA Protein Assay Kit (23228; Thermo Fisher Scientific), according to the manufacturer's instruction. Immunoblotting was performed for superoxide dismutase 2 (rabbit polyclonal IgG; 1:2000 dilution; ab13533; Abcam), catalase (rabbit monoclonal IgG; 1:1000 dilution; D4P7B#12980; Cell Signaling Technology, Danvers, MA), glutathione peroxidase 1 (rabbit polyclonal IgG; 1:2000 dilution; ab22064; Abcam), matrix metalloprotease (MMP)-2 (rabbit monoclonal IgG; 1:2000 dilution; D4M2N; Cell Signaling Technology), MMP-9 (rabbit polyclonal IgG; 1:1000 dilution; ab38898; Abcam), MMP-7 (rabbit monoclonal IgG; 1:1000 dilution; ab207299; Abcam), TGF-β1 (mouse monoclonal IgG; 1:1000 dilution; Ma5-18023; Thermo Fisher Scientific), α-SMA (rabbit polyclonal IgG; 1:1000 dilution; ab7817; Abcam), E-cadherin (rabbit monoclonal IgG; 1:2000 dilution; 24E10#3195; Cell Signaling Technology), N-cadherin (D4R1H; Cell Signaling Technology), and vimentin (ab24525; Abcam). The antigen-antibody complex was detected by SuperSignal chemiluminescent substrate (VJ311133; Thermo Fisher Scientific), according to the manufacturer's instruction. β-Actin antibody (sc-47778; Santa Cruz Biotechnology, Dallas, TX) was used for the protein normalization. Images of protein bands were acquired using a digital photographic scanner, GT-X750 (Seiko Epson Corp., Los Alamitos, CA), and were quantified using ImageJ software version 1.4.3.67.

Enzyme-Linked Immunosorbent Assay

Macaque's lung tissue homogenate of saline, SIV, Mor, and SIV + Mor groups was used to detect tumor necrosis factor-α and IL-1β using enzyme-linked immunosorbent assay kit (BMS223-4 and BMS224-2; Thermo Fischer Scientific), according to the manufacturer's instructions.

Statistical Analysis

The data are represented as means ± SEM. The statistical significance was analyzed by one-way analysis of variance, followed by Tukey multiple comparisons test using the GraphPad Prism Software version 5 (Boston, MA). Statistical analysis was performed, where $P < 0.05$ was considered statistically significant.

Results

Histopathologic Changes in the Lungs of Morphine-Exposed, SIV-Infected Macaques

The histopathologic changes in the lungs of macaques were analyzed by hematoxylin and eosin staining (Figure 1A). Normal distal lung morphology with archetypal alveolar spaces was observed in the saline control group (Figure 1A). However, SIV-infected and uninfected Mor-exposed macaques exhibited severe distortion of lung morphology, consisting of diffuse fibrous areas and obscured alveolar framework with thick scars. Inflammation-related tissue thickening with infiltration of immune cells into the interstitium was observed in SIV-infected macaque lungs (Figure 1A). Distorted architecture with honeycomb structures, consisting of enlarged airspaces lined by bronchial epithelium frequently filled with mucus and inflammatory cells, was evident in Mor alone (Figure 1A) and SIV + Mor (Figure 1A) macaque lungs. Fibroblastic foci, consisting of small dome-shaped interstitial collection of myofibroblasts, were observed in both Mor alone and SIV + Mor groups of macaque lungs. Large contiguous fibrotic masses with more frequent honeycomb and fibroblast foci, along with focal alveolar as well as interstitial damage, were found in all of the animals in SIV + Mor groups. The histopathologic scores are provided in Figure 1B, which shows that inflammation-related pathologic changes were high in SIV alone group of macaques ($^{*}P < 0.05$ versus saline; $^{\dagger}P < 0.05$ versus Mor; $^{\ddagger}P < 0.05$ versus SIV + Mor). SIV lung viral loads of all the chronically infected macaques (both SIV alone and SIV + Mor) were stable at 10^5 to 10^7 copies/μg of RNA (Table 1). Having found fibrotic changes in the lungs of experimental macaques, the study next analyzed the collagen deposition in each lung section by Masson trichrome staining. Representative micrographs are shown in Figure 1, C and D. Normal alveolar spaces with no signs of disease and typically low amounts of collagen were observed in the saline group (Figure 1C). Thickened alveolar septa, with some accumulation of pulmonary interstitial cells and collagen, were evident in SIV alone group (Figure 1C). Damaged alveolar structures and disorderly arranged lung parenchyma, with higher accumulation of interstitial collagen, were found in Mor alone group (Figure 1C). However, multifocal fibroblast clusters with massive accumulation of interstitial collagen were evident in the lungs of the SIV + Mor group (Figure 1D). Figure 1D represents the detailed assessment of collagen in the proximal and distal bronchiolar region of experimental macaque lungs. Collagen deposition was significantly high in the proximal bronchiolar region of SIV + Mor group (Figure 1D). Interestingly, more collagen deposition was found in the distal bronchiolar region of Mor alone and SIV + Mor group of macaque lungs (Figure 1D). Morphometric analysis was performed by calculating the percentage area of aniline blue–stained collagen fibers to estimate the degree of fibrosis. There was a significant

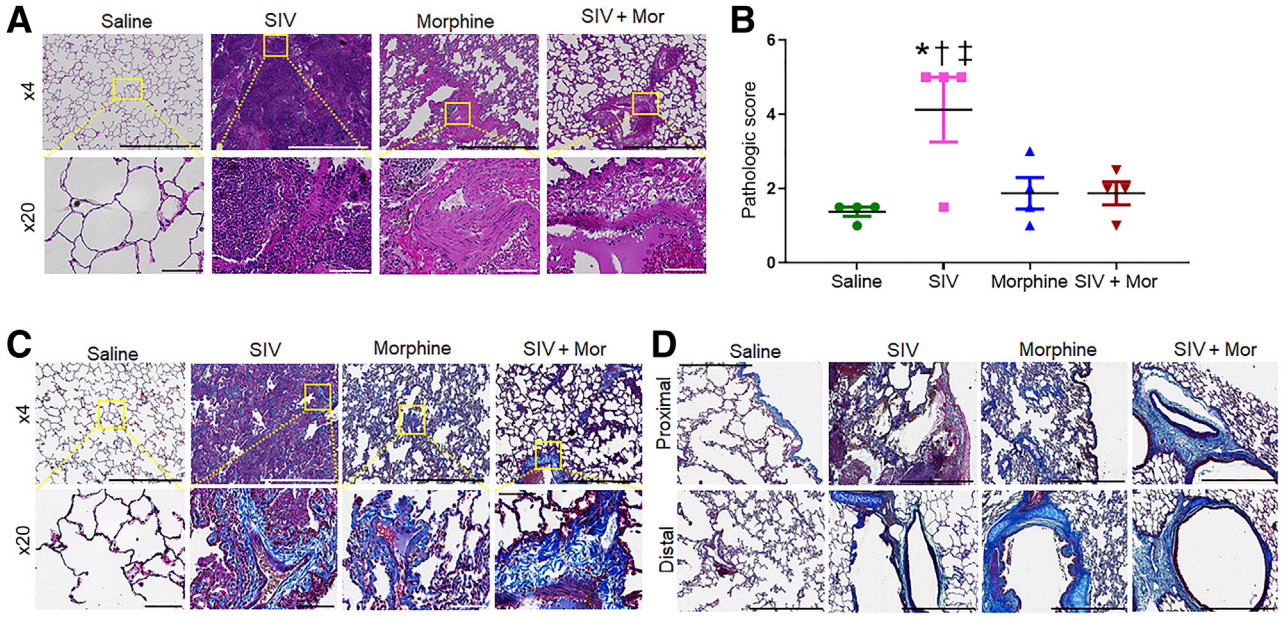

Figure 1 Pathologic analysis of the lung tissue. **A:** Hematoxylin and eosin (H&E) staining to examine lung pathology in saline, SIV, morphine (Mor), and SIV + Mor groups of macaques. **Top panels:** H&E-stained sections. **Bottom panels:** H&E-stained sections. **B:** Histopathologic scores of the different treatment groups. Immune cell infiltration was scored in macaque lungs stained with H&E. One-way analysis of variance, followed by Tukey multiple comparison test, was used to determine the statistical significance. **C:** Masson trichrome staining in lung tissues of experimental macaques. **Top panels:** Masson trichrome–stained sections. **Bottom panels:** Masson trichrome–stained sections. **D:** Masson trichrome staining in the proximal bronchioles (**top panels**) and distal bronchioles (**bottom panels**) of the experimental macaque lung tissues. Values represent the means ± SEM (**B**). $^{*}P < 0.05$ versus saline; $^{\dagger}P < 0.05$ versus Mor; $^{\ddagger}P < 0.05$ versus SIV + Mor. Scale bars: 1000 μm (**A** and **C**, **top panels**, and **D**); 100 μm (**A** and **C**, **bottom panels**). Original magnification: ×4 (**A** and **C**, **top panels**, and **D**); ×20 (**A** and **C**, **bottom panels**).

increase in the percentage area of collagen fibers in SIV + Mor group compared with the saline ($P < 0.05$), SIV ($P < 0.05$), and Mor ($P < 0.05$) groups. As expected, SIV alone ($P < 0.05$) and Mor alone ($P < 0.05$) groups also exhibited more collagen accumulation compared with saline control group (Supplemental Figure S1).

Increased Oxidative Stress in the Lungs of Morphine-Exposed, SIV-Infected Macaques

Several lines of evidence suggest that HIV infection causes pronounced oxidative stress.[19,20] To determine whether oxidative stress plays a significant role in SIV-induced PF, the expression of 4HNE, the end product of lipid peroxidation,[21] was examined in SIV- and/or Mor-exposed macaques. Immunofluorescence analysis of 4HNE in lung tissues indicated that both SIV and Mor independently increased the 4HNE levels that were further up-regulated in SIV + Mor lungs ($^{*}P < 0.05$ versus saline, $^{\dagger}P < 0.05$ versus SIV, and $^{\ddagger}P < 0.05$ versus Mor; immunofluorescence and quantification are shown) (Figure 2, A and B). Interestingly, the 4HNE adducts were localized predominantly in the cytoplasm of bronchial epithelial cells, and the expression was low in the cytoplasm of alveolar epithelial cells. Changes associated with SIV- and Mor-induced expression of 4HNE were also evident by Western blot analysis (Figure 2, C and D). To strengthen the inference that SIV/Mor affects the oxidation-reduction status of macaque lungs, the expression profile of antioxidant enzymes, including superoxide dismutase 2, was assessed. As shown in Figure 2E, a significant down-regulation of the enzyme was observed in macaque lungs exposed to SIV and Mor compared with saline ($^{*}P < 0.05$), SIV ($^{\dagger}P < 0.05$), and Mor ($^{\ddagger}P < 0.05$) groups of macaques. Similarly, Western blot analysis indicated that the levels of antioxidant enzymes catalase ($^{\dagger}P < 0.05$ versus SIV, and $^{\ddagger}P < 0.05$ versus Mor) and glutathione peroxidase 1 ($^{\dagger}P < 0.05$ versus SIV, and $^{\ddagger}P < 0.05$ versus Mor) were significantly reduced in SIV + Mor–exposed animals (Figure 2, E and F). However, interestingly, the level of these enzymes was independently up-regulated either by SIV exposure or by Mor dependence (Figure 2E). This might reflect an early attempt

Table 1 Representing the Viral Load of SIVmac251 in Lung Tissues of SIV Alone and SIV + Mor Group of Macaques

Lung tissue RNA viral loads		
Animal ID	Treatment	SIV copies/μg RNA
14T004	SIV	314,988,969
15N223	SIV	974,530
14X006	SIV	53,248,195
12N067	SIV	125,550
14X002	SIV + Mor	708,435
13T005	SIV + Mor	539,564
14X043	SIV + Mor	324,147

ID, identifier; Mor, morphine.

by the organism to compensate for the potential antioxidant milieu induced by the treatments. For example, vascular endothelial growth factor is important to mend lung injuries, and early or subtoxic exposure to cigarette smoke increases vascular endothelial growth factor.[22] However, chronic emphysema is associated with reduced levels of vascular endothelial growth factor in the lung.[23,24] Together, these results suggest that SIV and Mor may lead to lung injury through oxidative stress by changing the oxidation-reduction phenotype of the lung.

Increased Inflammation and Matrix Degradation in the Lungs of Morphine-Exposed, SIV-Infected Macaques

Because oxidative stress promotes PF by activating proinflammatory cytokines,[25,26] the study sought to examine the expression of proinflammatory cytokines in SIV/Mor-exposed macaque lungs. As examined by the enzyme-linked immunosorbent assay, the protein content of tumor necrosis factor-α and IL-1β was significantly elevated in all the treatment groups, with the greatest increase in the SIV alone group. The SIV group showed significant difference compared to saline, morphine, and SIV + Mor ($^{*,\dagger,\ddagger}P < 0.05$) (Figure 3, A and B). Considering that inflammatory cells may impact the pathogenesis of PF, the expression profile of MMPs was analyzed next, as oxidative stress and inflammation lead to degradation of ECM through the up-regulation of MMPs. MMPs, such as MMP-2, MMP-7, and MMP-9, degrade ECM and affect the structural integrity of pulmonary tissues in both experimental and clinical fibrotic lung pathologies.[27–29] Western blot analysis of the lungs indicated that MMP-2 and MMP-9 levels were significantly up-regulated in all treatment groups, with the largest increase in the SIV + Mor group. MMP-2 was significantly up-regulated in the SIV + Mor group compared to saline/morphine alone, while MMP-9 was significantly up-regulated in the SIV + Mor group compared to saline alone ($^{*}P < 0.05$ and $^{\ddagger}P < 0.05$, respectively) (Figure 3, C–E). Analogous results were observed with gelatin zymography analysis of the lung tissue homogenates from these groups (Figure 3F). Apart from MMP-2/MMP-9, matrilysin (MMP-7) is believed to play a central role in the pathogenesis of PF, as it is considered a potential peripheral blood biomarker in patients with PF.[27] As seen in Figure 3, G and H, SIV ($^{*}P < 0.05$) and Mor ($^{\dagger}P < 0.05$) independently increased MMP-7 levels compared to saline group; however, the levels of MMP-7

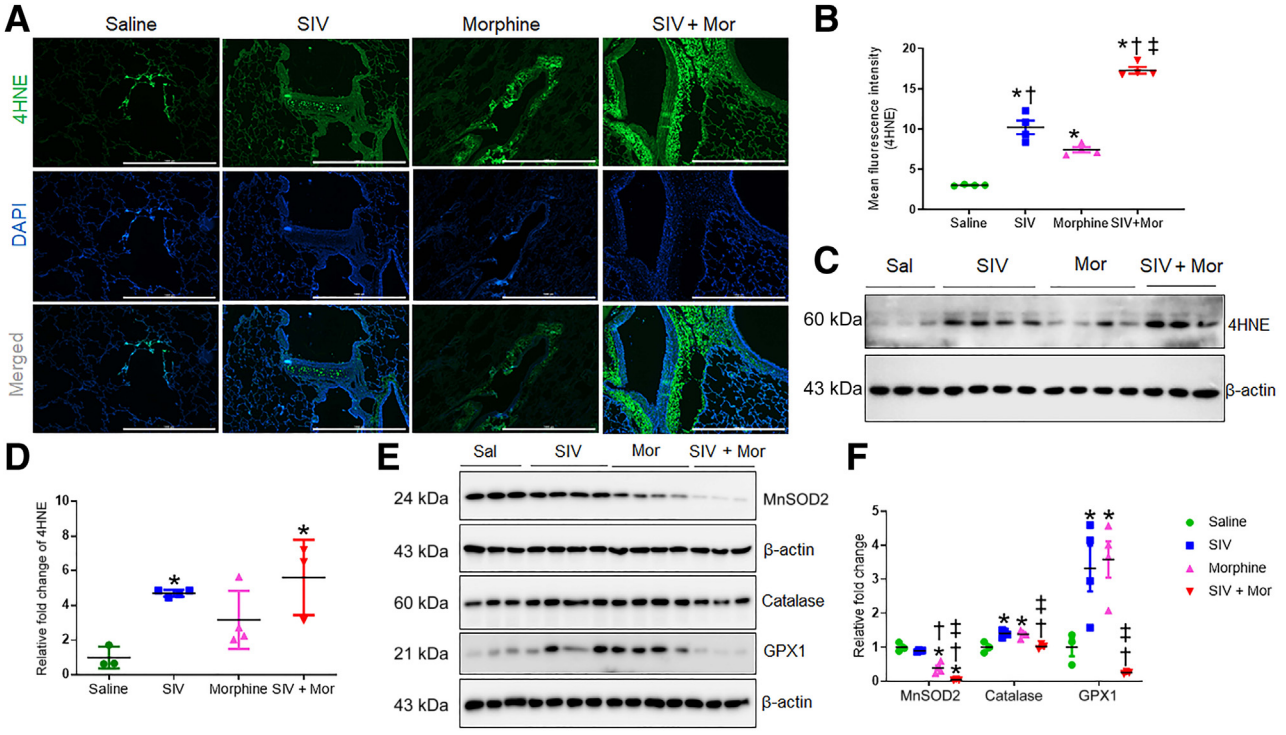

Figure 2 Increased oxidative stress in lungs of morphine (Mor)–exposed, SIV-infected macaques. **A:** Representative immunohistochemistry photomicrographs showing expression of 4-hydroxynonenal (4HNE) in lung tissues of morphine-exposed, SIV-infected macaques. **B:** Quantitative analysis of mean fluorescence intensity was performed in minimum 10 fields from four macaques. **C:** Western blot analysis showing expression of 4HNE in lung tissues of Mor-exposed, SIV-infected macaques. **D:** Quantitative analysis of relative fold change of 4HNE expression. **E:** Western blot analysis showing expression of superoxide dismutase 2 (MnSOD2), catalase, and glutathione peroxidase 1 (GPX1) in lung tissues of morphine-exposed, SIV-infected macaques. **F:** Quantitative analysis of relative fold change of protein expression. One-way analysis of variance, followed by Tukey multiple comparison test, was used to determine the statistical significance (**B**, **D**, and **F**). Values represent the means ± SEM (**B**, **D**, and **F**). $^{*}P < 0.05$ versus saline (Sal); $^{\dagger}P < 0.05$ versus SIV; $^{\ddagger}P < 0.05$ versus Mor. Scale bars = 1000 μm (**A**). Original magnification, ×4 (**A**).

were increased further by a combination of SIV + Mor ($^{\dagger}P < 0.05$) compared to morphine alone. These results suggest that SIV and Mor increase the concentrations of MMP-2, MMP-7, and MMP-9, which are likely to contribute to the increased chronic obstructive pulmonary disease and PF in PWH.

Morphine Dependence Increases the Expression of Profibrotic Transforming Growth Factor-β1 in SIV-Infected Macaque Lungs

TGF-β1 plays a crucial role in promoting lung fibrosis.[30] Therefore, the study determined the expression of TGF-β1 in macaque lungs exposed to SIV and/or morphine. As shown in Figure 4, A and B, Western blot analysis indicated that SIV and Mor independently significantly increased the expression of TGF-β1 over the control lungs ($^{*}P < 0.05$). Moreover, the expression was further increased in the SIV + Mor group ($^{*}P < 0.05$ versus saline, $^{\dagger}P < 0.05$ versus SIV, and $^{\ddagger}P < 0.05$ versus Mor). Similarly, the immunofluorescence analysis also showed similar changes in the expression of TGF-β1 in various experimental groups (Figure 4, C–E). TGF-β1 in the lung is primarily produced by the alveolar macrophages.[31,32] Therefore, the study determined the contribution of alveolar macrophages to the overproduction of TGF-β1. The lung tissue sections were stained for TGF-β1 and costained with the macrophage marker CD64. Indeed, the TGF-β1 staining largely colocalized with the CD64 marker in the lungs, and the expression was highest in the SIV + Mor–exposed lungs (Figure 4C).

Increased Fibroblast Proliferation and Myofibroblast Differentiation in Morphine-Exposed, SIV-Infected Rhesus Macaques

Fibroblast foci are the leading edge of PF pathogenesis and represent the differentiation of fibroblasts to myofibroblasts.[33] To ascertain the proliferation and differentiation of fibroblasts, the study examined the differentiation markers on the macaque lungs by Western blot and immunofluorescence. Expression of the proliferation marker Ki-67 was negligible in the nuclei of the control lungs. However, Ki-67 expression was significantly up-regulated in SIV, Mor, and SIV + Mor lungs compared to saline group ($^{*}P < 0.05$); in the latter (SIV + Mor), expression was higher than in the SIV or Mor groups ($^{\dagger, \ddagger}P < 0.05$) (Figure 5, A and B). Similarly, α-SMA

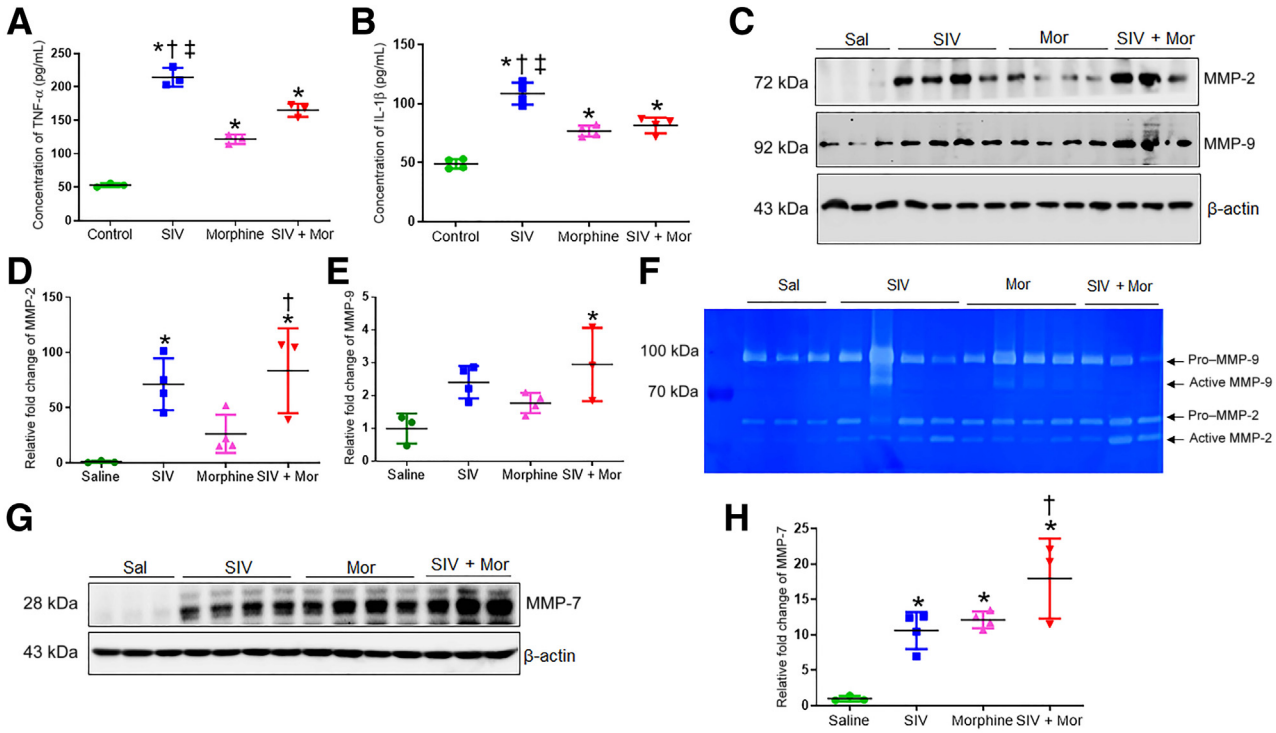

Figure 3 Increased inflammation and matrix degradation in lungs of morphine (Mor)–exposed, SIV-infected macaques. **A** and **B:** Enzyme-linked immunosorbent assay showing expression of tumor necrosis factor (TNF)-α and IL-1β in lung tissues of Mor-exposed, SIV-infected macaques. **C:** Western blot analysis showing expression of matrix metalloproteinase (MMP)-2 and MMP-9 in lung tissues of morphine-exposed, SIV-infected macaques. **D** and **E:** Quantitative analysis of relative fold change of MMP-2 and MMP-9 expression. **F:** Gelatin zymography analysis showing the expression of MMP-2 and MMP-9 in lung tissues of morphine-exposed, SIV-infected macaques. **G:** Western blot analysis showing expression of MMP-7 in lung tissues of morphine-exposed, SIV-infected macaques. **H:** Quantitative analysis of relative fold change of MMP-7 expression. One-way analysis of variance, followed by Tukey multiple comparison test, was used to determine the statistical significance (**A**, **B**, **D**, **E**, and **H**). Values represent the means ± SEM (**A**, **B**, **D**, **E**, and **H**). $^{*}P < 0.05$ versus saline (Sal); $^{\dagger}P < 0.05$ versus Mor; $^{\ddagger}P < 0.05$ versus SIV + Mor.

exhibited an analogous increase in the lungs as indicated by immunofluorescence (Figure 5, C and D) and Western blot (Figure 5, E and F). Using immunofluorescence localization, the study found that Ki-67–positive proliferating fibroblasts were localized within areas of interstitial fibrosis and away from fibroblast foci (Figure 5G). Myofibroblasts within the fibroblast foci expressed negligible antigen Ki-67 (Figure 5G). To validate this finding, lung tissue sections were costained with vimentin, along with Ki-67 and α-SMA. As shown in Figure 5H, α-SMA–positive cells in fibroblast foci that colocalized with vimentin were negative for Ki-67 expression. Ki-67–positive cells in the interstitial areas were colocalized with vimentin (Figure 5H), which confirmed that proliferating fibroblasts were localized in the interstitial fibrotic area and myofibroblasts in the fibroblast foci were less proliferating.

Increased Epithelial-Mesenchymal Transition in the Lungs of Morphine-Exposed, SIV-Infected Rhesus Macaques

Fibroblastic foci in the lung are characterized by vigorous proliferation and migration of mesenchymal cells through EMT, leading to an abnormal accumulation of ECM. The EMT is a biological process in which nonmotile epithelial cells change to a mesenchymal phenotype and the hallmark of EMT is the loss of epithelial surface markers, most notably E-cadherin, and the acquisition of mesenchymal markers, including vimentin and N-cadherin,[34] that leads to cell migration, proliferation, and adhesion,[35] promoting lung diseases, such as PF. Moreover, the lung epithelial/endothelial cell barriers form the tight junctions that require the participation of tight junction proteins, including claudins. The loss of claudins encourages diseases such as PF and chronic obstructive pulmonary disease in the lung.[36] The expression of the endothelial marker claudin-5 is reduced in the alveoli in interstitial pneumonitis in patients with HIV.[37] Therefore, whether SIV/Mor affected the expression of E-cadherin and N-cadherin, vimentin, and claudin-5 was studied next. As seen in the Western blot in Figure 6, A–D, compared with control macaque lungs, SIV and Mor significantly decreased E-cadherin and increased N-cadherin and vimentin, indicating that the treatments promoted EMT. Moreover, the combination of SIV and Mor (SIV + Mor) exaggerated these EMT indexes. Furthermore, examination of the immunofluorescence data indicates that SIV and Mor, independently and collectively, reduce the expression of claudin-5 (Figure 6, E and F). Together, these results suggest that SIV and Mor dysregulate the EMT and the lung alveolar tight junctions, which may encourage

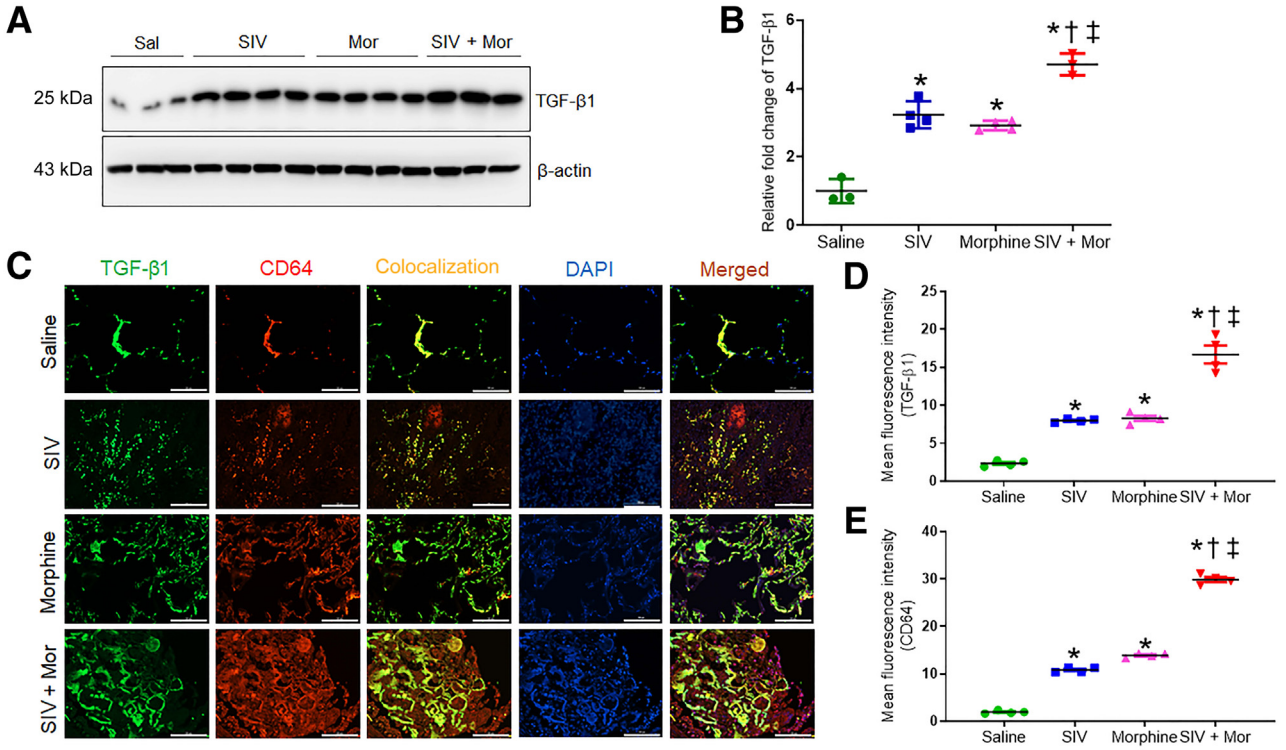

Figure 4 Increased expression of transforming growth factor (TGF)-β1 in lungs of morphine (Mor)–exposed, SIV-infected macaques. **A:** Western blot showing expression of TGF-β1 in lung tissues of Mor-exposed, SIV-infected macaques. **B:** Quantitative analysis of relative fold change of TGF-β1 expression. **C:** Representative immunohistochemistry photomicrographs showing expression of TGF-β1 and CD64 in lung tissues of Mor-exposed, SIV-infected macaques. **D** and **E:** Quantitative analysis of mean fluorescence intensity was performed in minimum 10 fields from four macaques. One-way analysis of variance, followed by Tukey multiple comparison test, was used to determine the statistical significance (**B**, **D**, and **E**). Values represent the means ± SEM (**B**, **D**, and **E**). $^{*}P < 0.05$ versus saline (Sal); $^{\dagger}P < 0.05$ versus SIV; $^{\ddagger}P < 0.05$ versus Mor. Scale bars = 100 μm (**C**). Original magnification, ×20 (**C**).

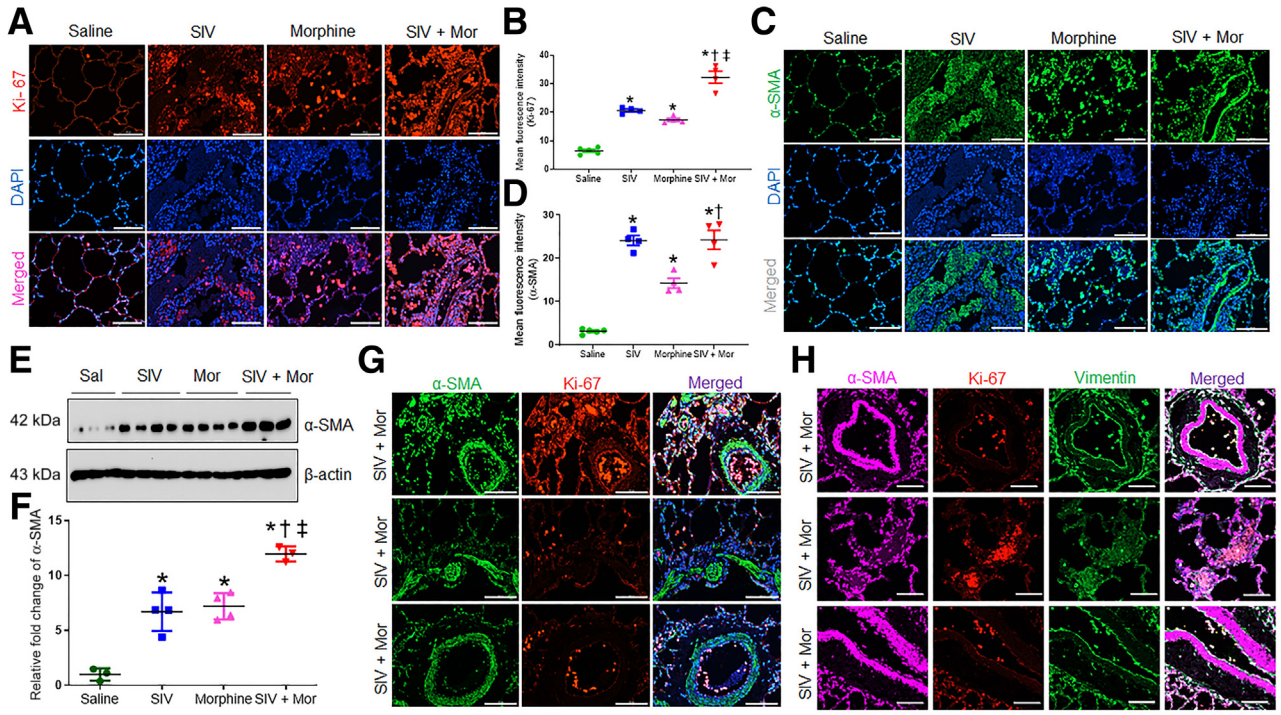

Figure 5 Increased fibroblast proliferation and myofibroblast differentiation in morphine (Mor)—exposed, SIV-infected rhesus macaques. **A** and **C:** Representative immunohistochemistry photomicrographs showing expression of Ki-67 (**A**) and α-smooth muscle actin (α-SMA; **C**) in lung tissues of morphine-exposed, SIV-infected macaques. **B** and **D:** Quantitative analysis of mean fluorescence intensity was performed in minimum 10 fields from four macaques. **E:** Western blot showing expression of α-SMA in lung tissues of Mor-exposed, SIV-infected macaques. **F:** Quantitative analysis of relative fold change of α-SMA expression. **G:** Representative immunohistochemistry photomicrographs showing the colocalization of Ki-67 and α-SMA in lung tissues of macaques from SIV + Mor group. **H:** Representative immunohistochemistry photomicrographs showing the colocalization of vimentin, Ki-67, and α-SMA in lung tissues of macaques from SIV + Mor group. One-way analysis of variance, followed by Tukey multiple comparison test, was used to determine the statistical significance (**B**, **D**, and **F**). Values represent the means ± SEM (**B**, **D**, and **F**). $^{*}P < 0.05$ versus saline (Sal); $^{\dagger}P < 0.05$ versus SIV; $^{\ddagger}P < 0.05$ versus Mor. Scale bars = 100 μm (**A**, **C**, **G**, and **H**). Original magnification, ×20 (**A**, **C**, **G**, and **H**).

fibrotic lung diseases. These processes are further exacerbated in the lungs exposed to both SIV + Mor.

Discussion

Pulmonary complications remain a substantial cause of morbidity and mortality in individuals with HIV. The fundamental mechanisms for the increased rates of pulmonary diseases in PWH are multifactorial. Earlier studies on SIV-infected rhesus macaques have shown altered pulmonary immunity with enhanced inflammation,[38] minimal cell death of virus-infected alveolar macrophages to facilitate HIV persistence, and promotion of lung damage.[39] Interestingly, morphine was found to potentiate the SIV-mediated pulmonary arteriopathy in rhesus macaques.[16] However, the effect of morphine and SIV interactions in inducing pulmonary fibrosis is yet to be revealed. In this context, this study used archival lung tissues from Mor-dependent SIV-infected rhesus macaques to explore the effect of Mor and SIV interaction on inducing fibrotic changes in the lungs. The study provided morphologic and molecular evidence for the induction of pulmonary fibrosis with increased accumulation of interstitial collagen and presence of honeycombing and fibroblast foci in the lungs of SIV-infected rhesus macaques exposed to morphine. To the best of our knowledge, this is the first study to report the incidence of pulmonary fibrosis in the rhesus macaque model of SIV infection and Mor dependence.

Mor dependence resulted in the formation of large contiguous fibrotic masses with honeycombing filled with inflammatory cells and fibroblast foci with abundant myofibroblasts and massive accumulation of interstitial collagen in SIV-infected macaque lungs. Numerous lines of evidence show that HIV infection triggers pronounced oxidative stress with a reduction of total antioxidant capacity in the lungs.[40] Interestingly, Mor interaction with SIV/simian HIV infection causes higher oxidative tissue injury in rhesus macaques.[41] In addition to macaques, abnormal oxidant/antioxidant balance is also evident in PWH, which may play a significant role in inducing lung damage.[26] A consequence of such increased oxidative burden may be lipid peroxidation in the lungs.[42] This study showed increased levels of 4HNE adducts, a highly reactive diffusible product of lipid peroxidation, in the bronchial epithelial cells of SIV-

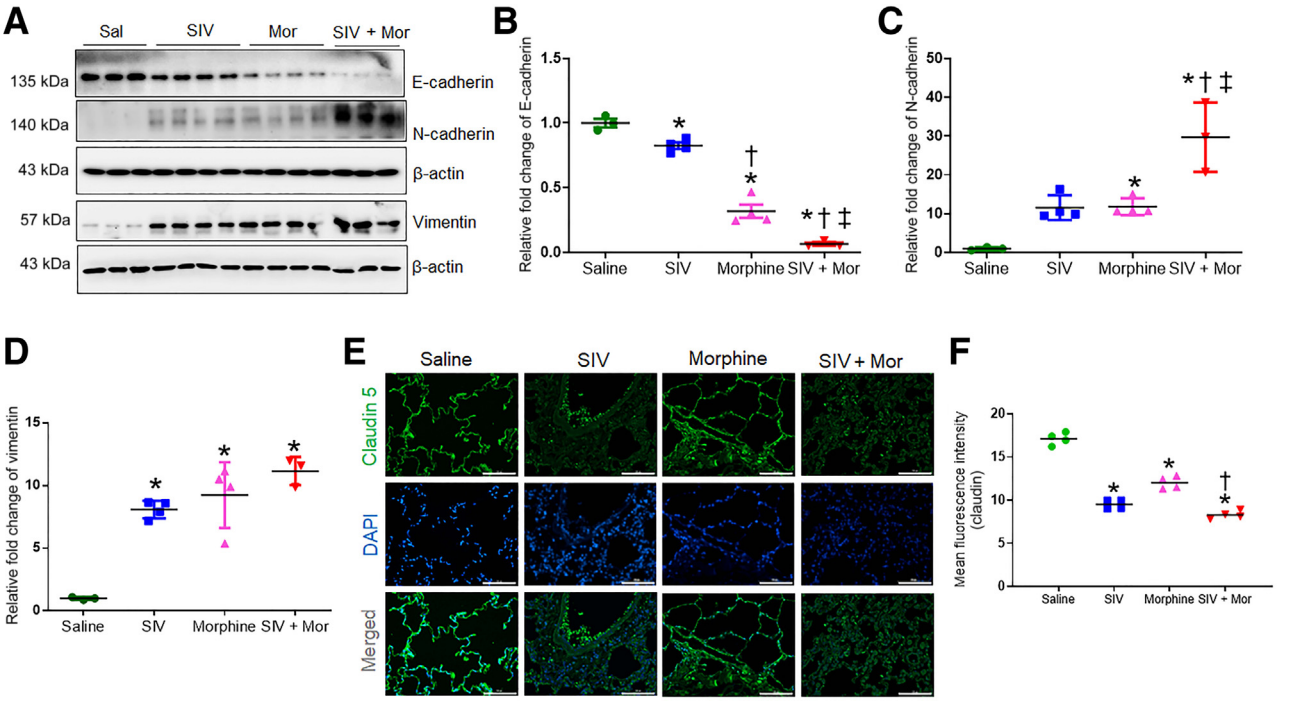

Figure 6 Increased epithelial-mesenchymal transition in the lungs of morphine (Mor)—exposed, SIV-infected rhesus macaque. **A:** Western blot analysis showing expression of E-cadherin, N-cadherin, and vimentin in lung tissues of morphine-exposed, SIV-infected macaques. **B**—**D:** Quantitative analysis of relative fold change of protein expression. **E:** Representative immunohistochemistry photomicrographs showing expression of claudin 5 in lung tissues of morphine-exposed, SIV-infected macaques. **F:** Quantitative analysis of mean fluorescence intensity was performed in minimum 10 fields from four macaques. One-way analysis of variance, followed by Tukey multiple comparison test, was used to determine the statistical significance (**B**—**D** and **F**). Values represent the means ± SEM (**B**—**D** and **F**). *$P < 0.05$ versus saline (Sal); †$P < 0.05$ versus SIV; ‡$P < 0.05$ versus Mor. Scale bars = 100 μm (**E**). Original magnification, ×20 (**E**).

infected macaques with chronic dependence to Mor. To evaluate the status of pulmonary antioxidant protection during SIV infection, the expression of antioxidant enzymes was analyzed. There was a dramatic decrease in the expression of antioxidants in the lungs of SIV + Mor group of macaques. However, there was a significant increase in the expression of catalase and glutathione peroxidase 1 in SIV- or Mor-treated macaque lungs. Persistent oxidative stress diminishes the potential of antioxidants to be expressed and imposes an imbalance between the production of oxidants and antioxidants in the lungs. This could be the possible reason for the enhanced expression of catalase and glutathione peroxidase 1 in SIV or Mor groups, and diminished expression of these antioxidants in SIV + Mor group of macaques. A recent study has demonstrated the pathogenic role of inflammatory cytokines that up-regulated the expression of MMPs in the lungs of patients with HIV who developed emphysema.[43] Up-regulated expression of MMPs play an important role in the development of PF. Among many different MMPs, MMP-2 and MMP-9 show increased activity in pulmonary diseases, including PF.[44] Herein, the study found that increased activity of MMPs is positively correlated to the pathogenesis and progression of PF on SIV infection and Mor dependence. The variability in the expression levels of MMPs and cytokines among the various macaque groups could be due to limitation in the number of animals in each group. It is possible that morphine dependence establishes a fibrotic phenotype that could occlude the inflammatory responses. It is also possible that although some pathways could be common, the two agents could also induce two distinct pathways to induce pathogenesis, which over time become distinct entities. Longitudinal assessment of disease condition in the context of morphine and/or SIV could lead to a better understanding of these pathways.

Overwhelming evidence highlights TGF-β1 as the most potent inducer of fibrosis by enhancing ECM production, matrix degradation, and collagen accumulation.[45] Wiercińska-Drapalo et al[46] investigated the possible relationship of circulating TGF-β1 with the clinical outcomes of HIV infection in a cohort of 66 patients. An almost twofold increase in the level of plasma TGF-β1 was observed in HIV-infected patients compared with healthy controls.[46] In an earlier study, Estes et al[14] found a parallel increase in immune activation, TGF-β1—positive regulatory T cells, and collagen 1 deposition in the lymphatic tissue of SIV-infected rhesus macaques. In addition to plasma and lymph nodes, TGF-β1 overproduction during pulmonary fibrogenesis is also evident from alveolar macrophages, bronchial epithelium, and alveolar epithelial cells.[31] The current finding supports these observations and suggests that Mor in combination with SIV enhances proliferation of

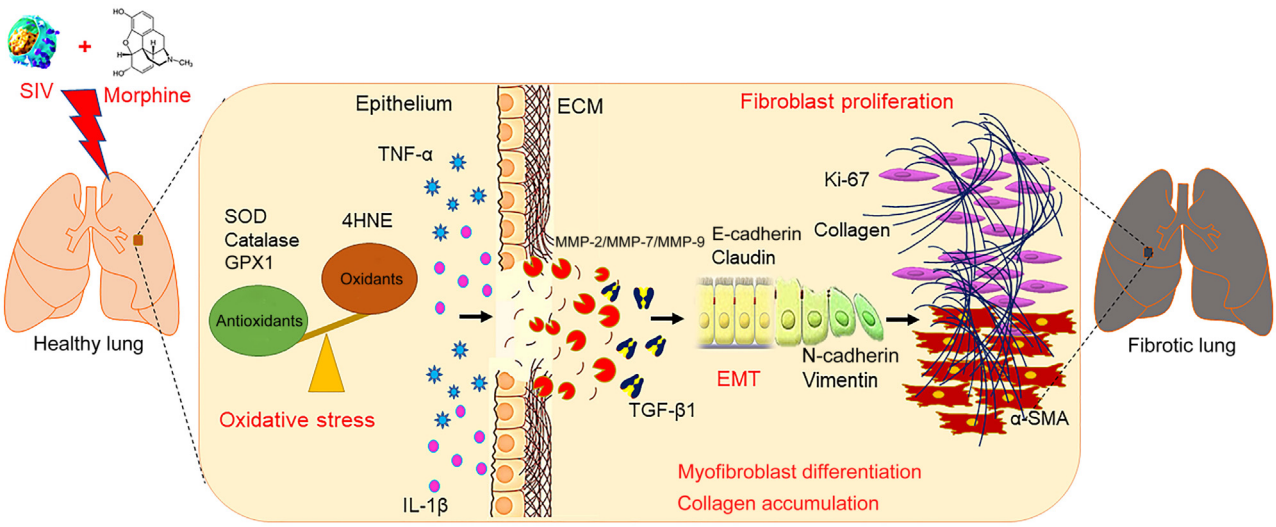

Figure 7 Schematic representation of the pathologic role of SIV and morphine in macaque lungs. SIV was shown to induce oxidative stress and inflammation with up-regulated expression of matrix-degrading enzymes matrix metalloproteinase (MMP)-2/MMP-9/MMP-7 in macaque lungs. These pathologic events may result in increased production of transforming growth factor (TGF)-β1 by alveolar macrophages, which further facilitate the induction of epithelial-mesenchymal transition (EMT) in lungs. Increased fibroblast proliferation and trans-differentiation of fibroblasts into myofibroblasts may result in the massive accumulation of interstitial collagen and fibrosis in experimental macaque lungs. Morphine was found to potentiate SIV-mediated pathologic changes in the lungs. ECM, extracellular matrix; GPX1, glutathione peroxidase 1; 4HNE, 4-hydroxynonenal; α-SMA, α-smooth muscle actin; SOD, superoxide dismutase; TNF-α, tumor necrosis factor-α.

fibroblasts, which could lead to an increase in the expression of TGF-β1 in macaque lungs. Although multiple cell types are involved in the pathogenesis of lung fibrosis, fibroblast proliferation and trans-differentiation of fibroblasts to myofibroblasts are considered as the key events in the initiation and progression of PF. In the context of fibrosis, TGF-β1 released by the injured alveolar epithelial cells or alveolar macrophages can cause trans-differentiation of fibroblast to myofibroblast that contributes to tissue remolding via overproduction of ECM proteins, cytokines, and specific growth factors.[47,48] Myofibroblasts are transiently present and orchestrate scar formation in normal acute wounds. However, persistent activation of myofibroblast at the site of injury results in excessive deposition of ECM. In accordance with the previous reports on PF, an abnormal proliferation of fibroblasts and their differentiated phenotype, myofibroblasts, was found herein in the experimental lung tissues.[49] The origin of these contractile α-SMA−positive myofibroblasts remains debated. Previous studies sought to explain and have proposed several theories for the origin of these cells, including the following: i) they are derived from proliferating and activated resident fibroblasts, ii) they are derived from type I or type II epithelial cells via the process of EMT, iii) they are derived from bone marrow−derived fibroblast, or iv) they are derived from pericytes in the lung interstitium.[50] Several studies have highlighted the best explanation for the increased myofibroblasts in the injured epithelial area, which is EMT, in which type I and type II epithelial cells lose their epithelial cell phenotype and acquire mesenchymal characteristics with increased motility that helps to escape the injured area. The current results substantiate the previous reports, where decreased expression of epithelial markers along with increased expression of mesenchymal markers were noted in the rodent model of PF.[51,52]

On the basis of these observations, we speculate that morphine significantly potentiates SIV-mediated fibrogenesis and progression of fibrosis in macaque lungs. Although the mechanistic underpinnings are not clearly defined in this study, it provides proof that Mor dependence enhances oxidative stress−mediated epithelial degeneration, the release of profibrotic TGF-β1, transactivation of myofibroblasts, and accumulation of interstitial collagen associated with SIV infection in macaque lungs (Figure 7). A better contemporary understanding of the burden of pulmonary complications associated with HIV infection is important for patient care and future research endeavors in this field. SIV and morphine show significant effects individually, and whether these are additive or synergistic is not clear. It is possible that although some pathways could be common, the two agents could also induce two distinct pathways to induce pathogenesis, which over time become distinct entities, both harmful to the subject. Longitudinal assessment of disease condition in the context of morphine and/or SIV could lead to a better understanding of these pathways. In addition, a recent publication also demonstrated that morphine can cause immune suppression in SIV-infected animals.[53]

Acknowledgments

We thank Drs. Palsamy Periyasamy, Guoku Hu, Muthukumar Kannan, Seema Singh, Sudipta Ray, Ernest Chivero, Annadurai Thangaraj, and Abiola Oladapo for helpful

discussions; and Natasha Ferguson for technical assistance and experiments with nonhuman primates.

Author Contributions

D.T.C. conceived and designed the study, performed the experiments, analyzed the data, and wrote the manuscript; S.S. designed the study, analyzed the data, and wrote the manuscript; S.C. performed SIV infection and morphine treatment in macaques and edited the manuscript; H.S.C. and M.S. interpreted data and edited the manuscript; T.A.W. performed histopathologic analysis, interpreted the data, and edited the manuscript; A.A. and S.N.B. performed viral load analysis and edited the manuscript; H.S.F. contributed to the macaque study and edited the manuscript; S.B. conceived, designed, and supervised the study, analyzed and interpreted the data, edited the manuscript, and acquired funding for the study.

Supplemental Data

Supplemental material for this article can be found at *http://doi.org/10.1016/j.ajpath.2022.12.016*.

References

1. Wallace JM, Hansen NI, Lavange L, Glassroth J, Browdy BL, Rosen MJ, Kvale PA, Mangura BT, Reichman LB, Hopewell PC; Pulmonary Complications of HIV Infection Study Group: Respiratory disease trends in the Pulmonary Complications of HIV Infection Study cohort. Am J Respir Crit Care Med 1997, 155:72–80
2. Drummond MB, Kirk GD: HIV-associated obstructive lung diseases: insights and implications for the clinician. Lancet Respir Med 2014, 2:583–592
3. Crothers K, Butt AA, Gibert CL, Rodriguez-Barradas MC, Crystal S, Justice AC; Veterans Aging Cohort 5 Project Team: Increased COPD among HIV-positive compared to HIV-negative veterans. Chest 2006, 130:1326–1333
4. ten Freyhaus H, Vogel D, Lehmann C, Kummerle T, Wyen C, Fatkenheuer G, Rosenkranz S: Echocardiographic screening for pulmonary arterial hypertension in HIV-positive patients. Infection 2014, 42:737–741
5. Sabin CA, Kunisaki KM, Bagkeris E, Post FA, Sachikonye M, Boffito M, Anderson J, Mallon P, Williams I, Vera JH, Johnson M, Babalis D, Winston A: Respiratory symptoms and chronic bronchitis in people with and without HIV infection. HIV Med 2021, 22:11–21
6. Kynyk JA, Parsons JP, Para MF, Koletar SL, Diaz PT, Mastronarde JG: HIV and asthma, is there an association? Respir Med 2012, 106:493–499
7. Crothers K, Huang L, Goulet JL, Goetz MB, Brown ST, Rodriguez-Barradas MC, Oursler KK, Rimland D, Gibert CL, Butt AA, Justice AC: HIV infection and risk for incident pulmonary diseases in the combination antiretroviral therapy era. Am J Respir Crit Care Med 2011, 183:388–395
8. Rabkin JG, McElhiney MC, Ferrando SJ: Mood and substance use disorders in older adults with HIV/AIDS: methodological issues and preliminary evidence. AIDS 2004, 18(Suppl 1):S43–S48
9. Gingo MR, George MP, Kessinger CJ, Lucht L, Rissler B, Weinman R, Slivka WA, McMahon DK, Wenzel SE, Sciurba FC, Morris A: Pulmonary function abnormalities in HIV-infected patients during the current antiretroviral therapy era. Am J Respir Crit Care Med 2010, 182:790–796
10. Liu YM, Nepali K, Liou JP: Idiopathic pulmonary fibrosis: current status, recent progress, and emerging targets. J Med Chem 2017, 60: 527–553
11. Mostafaei S, Sayad B, Azar MEF, Doroudian M, Hadifar S, Behrouzi A, Riahi P, Hussen BM, Bayat B, Nahand JS, Moghoofei M: The role of viral and bacterial infections in the pathogenesis of IPF: a systematic review and meta-analysis. Respir Res 2021, 22:53
12. Wynn TA: Integrating mechanisms of pulmonary fibrosis. J Exp Med 2011, 208:1339–1350
13. Willis BC, Liebler JM, Luby-Phelps K, Nicholson AG, Crandall ED, du Bois RM, Borok Z: Induction of epithelial-mesenchymal transition in alveolar epithelial cells by transforming growth factor-beta1: potential role in idiopathic pulmonary fibrosis. Am J Pathol 2005, 166: 1321–1332
14. Estes JD, Wietgrefe S, Schacker T, Southern P, Beilman G, Reilly C, Milush JM, Lifson JD, Sodora DL, Carlis JV, Haase AT: Simian immunodeficiency virus-induced lymphatic tissue fibrosis is mediated by transforming growth factor beta 1-positive regulatory T cells and begins in early infection. J Infect Dis 2007, 195: 551–561
15. Zeng M, Smith AJ, Wietgrefe SW, Southern PJ, Schacker TW, Reilly CS, Estes JD, Burton GF, Silvestri G, Lifson JD, Carlis JV, Haase AT: Cumulative mechanisms of lymphoid tissue fibrosis and T cell depletion in HIV-1 and SIV infections. J Clin Invest 2011, 121: 998–1008
16. Spikes L, Dalvi P, Tawfik O, Gu H, Voelkel NF, Cheney P, O'Brien-Ladner A, Dhillon NK: Enhanced pulmonary arteriopathy in simian immunodeficiency virus-infected macaques exposed to morphine. Am J Respir Crit Care Med 2012, 185:1235–1243
17. Acharya A, Olwenyi OA, Thurman M, Pandey K, Morsey BM, Lamberty B, Ferguson N, Callen S, Fang Q, Buch SJ, Fox HS, Byrareddy SN: Chronic morphine administration differentially modulates viral reservoirs in SIVmac251 infected rhesus macaque model. J Virol 2020, 95:e01657-20
18. Sil S, Singh S, Chemparathy DT, Chivero ET, Gordon L, Buch S: Astrocytes & astrocyte derived extracellular vesicles in morphine induced amyloidopathy: implications for cognitive deficits in opiate abusers. Aging Dis 2021, 12:1389–1408
19. Wanchu A, Rana SV, Pallikkuth S, Sachdeva RK: Short communication: oxidative stress in HIV-infected individuals: a cross-sectional study. AIDS Res Hum Retroviruses 2009, 25:1307–1311
20. Ivanov AV, Valuev-Elliston VT, Ivanova ON, Kochetkov SN, Starodubova ES, Bartosch B, Isaguliants MG: Oxidative stress during HIV infection: mechanisms and consequences. Oxid Med Cell Longev 2016, 2016:8910396
21. Rahman I, van Schadewijk AA, Crowther AJ, Hiemstra PS, Stolk J, MacNee W, De Boer WI: 4-Hydroxy-2-nonenal, a specific lipid peroxidation product, is elevated in lungs of patients with chronic obstructive pulmonary disease. Am J Respir Crit Care Med 2002, 166:490–495
22. Volpi G, Facchinetti F, Moretto N, Civelli M, Patacchini R: Cigarette smoke and alpha,beta-unsaturated aldehydes elicit VEGF release through the p38 MAPK pathway in human airway smooth muscle cells and lung fibroblasts. Br J Pharmacol 2011, 163:649–661
23. Tuder RM, Yun JH: Vascular endothelial growth factor of the lung: friend or foe. Curr Opin Pharmacol 2008, 8:255–260
24. Lee CG, Ma B, Takyar S, Ahangari F, Delacruz C, He CH, Elias JA: Studies of vascular endothelial growth factor in asthma and chronic obstructive pulmonary disease. Proc Am Thorac Soc 2011, 8: 512–515
25. Cheresh P, Kim SJ, Tulasiram S, Kamp DW: Oxidative stress and pulmonary fibrosis. Biochim Biophys Acta 2013, 1832:1028–1040
26. Victoni T, Barreto E, Lagente V, Carvalho VF: Oxidative imbalance as a crucial factor in inflammatory lung diseases: could antioxidant

treatment constitute a new therapeutic strategy? Oxid Med Cell Longev 2021, 2021:6646923
27. Rosas IO, Richards TJ, Konishi K, Zhang Y, Gibson K, Lokshin AE, Lindell KO, Cisneros J, Macdonald SD, Pardo A, Sciurba F, Dauber J, Selman M, Gochuico BR, Kaminski N: MMP1 and MMP7 as potential peripheral blood biomarkers in idiopathic pulmonary fibrosis. PLoS Med 2008, 5:e93
28. Kim JY, Choeng HC, Ahn C, Cho SH: Early and late changes of MMP-2 and MMP-9 in bleomycin-induced pulmonary fibrosis. Yonsei Med J 2009, 50:68−77
29. Zhang Y, Li Y, Ye Z, Ma H: Expression of matrix metalloproteinase-2, matrix metalloproteinase-9, tissue inhibitor of metalloproteinase-1, and changes in alveolar septa in patients with chronic obstructive pulmonary disease. Med Sci Monit 2020, 26: e925278
30. Wei Y, Kim TJ, Peng DH, Duan D, Gibbons DL, Yamauchi M, Jackson JR, Le Saux CJ, Calhoun C, Peters J, Derynck R, Backes BJ, Chapman HA: Fibroblast-specific inhibition of TGF-beta1 signaling attenuates lung and tumor fibrosis. J Clin Invest 2017, 127: 3675−3688
31. Khalil N, Bereznay O, Sporn M, Greenberg AH: Macrophage production of transforming growth factor beta and fibroblast collagen synthesis in chronic pulmonary inflammation. J Exp Med 1989, 170: 727−737
32. Fernandez IE, Eickelberg O: The impact of TGF-beta on lung fibrosis: from targeting to biomarkers. Proc Am Thorac Soc 2012, 9: 111−116
33. Wei P, Xie Y, Abel PW, Huang Y, Ma Q, Li L, Hao J, Wolff DW, Wei T, Tu Y: Transforming growth factor (TGF)-beta1-induced miR-133a inhibits myofibroblast differentiation and pulmonary fibrosis. Cell Death Dis 2019, 10:670
34. Serrano-Gomez SJ, Maziveyi M, Alahari SK: Regulation of epithelial-mesenchymal transition through epigenetic and post-translational modifications. Mol Cancer 2016, 15:18
35. Noronha C, Ribeiro AS, Taipa R, Castro DS, Reis J, Faria C, Paredes J: Cadherin expression and EMT: a focus on gliomas. Biomedicines 2021, 9:1328
36. Frank JA: Claudins and alveolar epithelial barrier function in the lung. Ann N Y Acad Sci 2012, 1257:175−183
37. Andras IE, Toborek M: HIV-1-induced alterations of claudin-5 expression at the blood-brain barrier level. Methods Mol Biol 2011, 762:355−370
38. Hunegnaw R, Mushtaq Z, Enyindah-Asonye G, Hoang T, Robert-Guroff M: Alveolar macrophage dysfunction and increased PD-1 expression during chronic SIV infection of rhesus macaques. Front Immunol 2019, 10:1537
39. Cai Y, Sugimoto C, Arainga M, Midkiff CC, Liu DX, Alvarez X, Lackner AA, Kim WK, Didier ES, Kuroda MJ: Preferential destruction of interstitial macrophages over alveolar macrophages as a cause of pulmonary disease in simian immunodeficiency virus-infected rhesus macaques. J Immunol 2015, 195:4884−4891
40. Awodele O, Olayemi SO, Nwite JA, Adeyemo TA: Investigation of the levels of oxidative stress parameters in HIV and HIV-TB co-infected patients. J Infect Dev Ctries 2012, 6:79−85
41. Perez-Casanova A, Husain K, Noel RJ Jr, Rivera-Amill V, Kumar A: Interaction of SIV/SHIV infection and morphine on plasma oxidant/antioxidant balance in macaque. Mol Cell Biochem 2008, 308: 169−175
42. Madebo T, Lindtjorn B, Aukrust P, Berge RK: Circulating antioxidants and lipid peroxidation products in untreated tuberculosis patients in Ethiopia. Am J Clin Nutr 2003, 78:117−122
43. Barjaktarevic IZ, Crystal RG, Kaner RJ: The role of interleukin-23 in the early development of emphysema in HIV1(+) smokers. J Immunol Res 2016, 2016:3463104
44. Craig VJ, Zhang L, Hagood JS, Owen CA: Matrix metalloproteinases as therapeutic targets for idiopathic pulmonary fibrosis. Am J Respir Cell Mol Biol 2015, 53:585−600
45. Thomas BJ, Kan OK, Loveland KL, Elias JA, Bardin PG: In the shadow of fibrosis: innate immune suppression mediated by transforming growth factor-beta. Am J Respir Cell Mol Biol 2016, 55:759−766
46. Wiercińska-Drapalo A, Flisiak R, Jaroszewicz J, Prokopowicz D: Increased plasma transforming growth factor-beta1 is associated with disease progression in HIV-1-infected patients. Viral Immunol 2004, 17:109−113
47. Vallee A, Lecarpentier Y: TGF-beta in fibrosis by acting as a conductor for contractile properties of myofibroblasts. Cell Biosci 2019, 9:98
48. Harris WT, Kelly DR, Zhou Y, Wang D, MacEwen M, Hagood JS, Clancy JP, Ambalavanan N, Sorscher EJ: Myofibroblast differentiation and enhanced TGF-B signaling in cystic fibrosis lung disease. PLoS One 2013, 8:e70196
49. Hill C, Li J, Liu D, Conforti F, Brereton CJ, Yao L, Zhou Y, Alzetani A, Chee SJ, Marshall BG, Fletcher SV, Hancock D, Ottensmeier CH, Steele AJ, Downward J, Richeldi L, Lu X, Davies DE, Jones MG, Wang Y: Autophagy inhibition-mediated epithelial-mesenchymal transition augments local myofibroblast differentiation in pulmonary fibrosis. Cell Death Dis 2019, 10:591
50. Scotton CJ, Chambers RC: Molecular targets in pulmonary fibrosis: the myofibroblast in focus. Chest 2007, 132:1311−1321
51. Divya T, Velavan B, Sudhandiran G: Regulation of transforming growth factor-beta/Smad-mediated epithelial-mesenchymal transition by celastrol provides protection against bleomycin-induced pulmonary fibrosis. Basic Clin Pharmacol Toxicol 2018, 123:122−129
52. Guo L, Xu JM, Liu L, Liu SM, Zhu R: Hypoxia-induced epithelial-mesenchymal transition is involved in bleomycin-induced lung fibrosis. Biomed Res Int 2015, 2015:232791
53. Fox HS, Niu M, Morsey BM, Lamberty BG, Emanuel K, Periyasamy P, Callen S, Acharya A, Kubik G, Eudy J, Guda C, Dyavar SR, Fletcher CV, Byrareddy SN, Buch S: Morphine suppresses peripheral responses and transforms brain myeloid gene expression to favor neuropathogenesis in SIV infection. Front Immunol 2022, 13:1012884